Journal of Chromatography A, 1218 (2011) 5449–5455

Contents lists available at ScienceDirect

Journal of Chromatography A

journal homepage: www.elsevier.com/locate/chroma

Modified Equilibrium-Dispersive Model for the interpretation of the efficiency of columns packed with core–shell particle

Joanna Kostka[a], Fabrice Gritti[b,c], Krzysztof Kaczmarski[a,*], Georges Guiochon[b,c,**]

[a] Department of Chemical and Process Engineering, Rzeszów University of Technology, 35-959 Rzeszów, Poland
[b] Department of Chemistry, University of Tennessee, Knoxville, TN 37996-1600, USA
[c] Division of Chemical Sciences, Oak Ridge National Laboratory, Oak Ridge, TN 37831, USA

ARTICLE INFO

Article history:
Received 9 April 2011
Received in revised form 3 June 2011
Accepted 6 June 2011
Available online 17 June 2011

Keywords:
Shell particles
Column efficiency
HETP
Apparent and axial dispersion
Van Deemter plot
Peak profiles

ABSTRACT

A modified Equilibrium Dispersive (ED) Model is proposed for the modeling of chromatographic processes in columns packed with shell-particle adsorbents and operated under very high pressures. This new model was validated on the basis of experimental results obtained with 2.1 mm × 150 mm columns packed with superficially porous 1.7 μm Kinetex-C_{18} particles and with classical columns packed with 1.7 μm BEH-C_{18} fully porous particles. The influence of the heat friction on the performance of these columns was analyzed by comparing the experimental and calculated peak profiles. Moreover a theoretical analysis of the influence the solid-core conductivity on the column efficiency was discussed.

1. Introduction

The current trend in chromatography still tends toward the achievement of higher efficiency and shorter analysis times. For this reason, manufacturers of packing materials are developing new kinds of finer silica particles. Traditionally, totally porous particles are used in HPLC. Now, various types of column packing are available and one of the new packing materials used is made of superficially porous core–shell particles. These particles are made of a solid, nonporous core surrounded by a porous shell. In recent years, manufacturers have prepared several generations of shell particles. Late 2006, Kirkland [1] prepared columns packed with Halo particles made of a 1.6 μm solid silica core surrounded by a 0.50 μm porous silica shell. These columns were exceptionally efficient, with reduced plate height around 1.5. In 2009, Phenomenex offered first 4.6 mm i.d. Kinetex columns packed with shell particles having similar characteristics and, later 2.1 mm Kinetex columns packed with 1.25 μm solid silica core surrounded by a 0.23 μm porous silica shell. Last year, Agilent commercialized columns packed with Poroshell 120 particles that have similar characteristics.

The experimental and theoretical analysis of the efficiency of columns packed with shell particles were discussed, among others in [2–7].

Gritti and Guiochon [2] investigated and compared the performance of 2.1 mm × 150 mm columns packed with 1.7 μm shell Kinetex-C_{18} and with totally porous 1.7 μm BEH-C_{18} particles. The solute was naphtho[2,3-α]pyrene. The reduced HETPs of two columns were measured in pure acetonitrile and aqueous solution of acetonitrile at 295 K. The HETP of both columns were similar, but the minimum was observed at a shorter reduced linear velocity for the column packed with totally porous particles than for the column packed with shell particles. These authors demonstrated that the negative effects of heat generated by viscous friction and of the radial temperature gradients are smaller for columns packed with shell particles than for columns packed with totally porous particles. At high velocities, the efficiency of Kinetex column depends less on the mobile phase velocity under still-air conditions. Hence, at high flow rates, the HETP plot of the Kinetex column increase more slowly than that of the BEH column. According to these authors this should be due to the larger thermal conductivity of shell particles, which contain a solid silica core occupying about 40% of the particle volume [2].

In this work, we used more powerful tools to interpret the results of the experiments described in [2]. The main goal of our

* Corresponding author. Tel.: +48 17 865 12 95; fax: +48 17 854 36 55.
** Corresponding author at: Department of Chemistry, University of Tennessee, Knoxville, TN 37996-1600, USA. Tel.: +1 865 974 0733; fax: +1 865 974 2667.
E-mail addresses: kkaczmarski@prz.edu.pl, kkaczmarski@prz.rzeszow.pl (K. Kaczmarski), guiochon@utk.edu (G. Guiochon).

0021-9673/$ – see front matter © 2011 Elsevier B.V. All rights reserved.
doi:10.1016/j.chroma.2011.06.019

work is to determine whether the larger effective conductivity of columns packed with inert core particles causes smaller loss of efficiency at high flow velocities.

2. Mathematical models

The mathematical model consists of three separate models: (1) a model of heat transfer, (2) a model for the mobile phase velocity distribution, and (3) a model of mass transfer. The first model expresses how the heat generated by viscous friction is evacuated from the column under steady-state conditions. The second model accounts for the distribution of the mobile phase velocity, which depends on the local temperature and pressure and is given by the equations of hydrodynamics in porous media. These two models are exactly the same as described in our previous papers [8,9] and will not be presented here. To solve a model of heat transfer and a model of mobile phase velocity distribution, the eluent density, its viscosity, its thermal expansion coefficient and its heat capacity as functions of pressure and temperature must be calculated. These values, as well as the effective thermal conductivity of the bed, were calculated according to correlations given in [9].

The third model of mass transfer accounts for the propagation of a compound band along a column that is no longer isothermal. The equilibrium constant depends on the local temperatures and pressures; so does the migration rate of a concentration. In this work we applied a modified Equilibrium-Dispersive (ED) Model for core–shell particles.

2.1. The mass balance equations

The mass balance equation of the ED model for column packed with shell particles and for isothermal column is written as follows [6]:

$$\frac{\partial c}{\partial t} + \frac{(1-\varepsilon_e)(1-\varepsilon_p)(1-q^3)}{\varepsilon_t}\frac{\partial q}{\partial t} + \frac{u}{\varepsilon_t}\frac{\partial c}{\partial x} = \frac{\varepsilon_e}{\varepsilon_t}D_L\frac{\partial^2 c}{\partial x^2} \quad (1)$$

where c and q are the analyte concentrations in the mobile and in the stationary phases (g/l), respectively, D_L is the axial dispersion coefficient (m^2/s), u (m/s) is the superficial velocity, ε_t, ε_e, and ε_p are the total, external and particle porosities, t is the time (s), $\rho = R_i/R_e$, where R_i, R_e are the inner and the external radius of the particles, respectively. It should be noticed that the particle porosity ε_p is referenced to the particle volume for totally porous adsorbent but only to the shell volume for core–shell particles.

For very high pressure drops the column is not isothermal because heat is generated by the friction of the eluent percolating the bed. The diffusion of this heat out of the column generates temperature gradients. Due to these axial and radial temperature gradients, the other physico-chemical parameters depend on the axial and the radial position. To take these into account the one dimensional ED model, Eq. (1), has to be replaced by its two dimensional versions:

$$\frac{\partial c}{\partial t} + \frac{(1-\varepsilon_e)(1-\varepsilon_p)(1-\rho^3)}{\varepsilon_t}\frac{\partial q}{\partial t} + \frac{1}{\varepsilon_t}\frac{\partial (uc)}{\partial x} = \frac{\partial}{\partial x}\left(D_{a,x}\frac{\partial c}{\partial x}\right) + \frac{1}{r}\frac{\partial}{\partial r}\left(rD_{a,r}\frac{\partial c}{\partial r}\right) \quad (2)$$

where $D_{a,x}$ and $D_{a,r}$ are the apparent axial and radial dispersion coefficients (m^2/s). Eq. (2) was solved assuming that initially there is no solute in the column. The solute is injected into the column during the time $t_{injection}$. The gradient of concentration at the column outlet, the column center and its wall region are equal to zero.

The total porosity is calculated from the equation [6]:

$$\varepsilon_t = \varepsilon_e + (1-\varepsilon_e)\varepsilon_p\left(1 - \frac{R_i^s}{R_e^s}\right) \quad (3)$$

In earlier papers [10], it was proved that the solution of the unidimensional ED model (without a radial term and with a constant mobile phase velocity), for totally porous adsorbent is compatible with the general rate model when the axial apparent dispersion coefficient is calculated from the following equation:

$$D_{a,x} = \frac{D_L\varepsilon_e}{\varepsilon_t} + \left(\frac{k_1}{1+k_1}\right)^2\frac{u^2 d_p}{\varepsilon_t\varepsilon_e F_e 6}\left[\frac{d_p}{10D_{eff}} + \frac{1}{k_{ext}}\right] \quad (4)$$

where

$$k_1 = F_e\left(\varepsilon_p + (1-\varepsilon_p)\frac{\partial q}{\partial c}\right); \quad F_e = \frac{1-\varepsilon_e}{\varepsilon_e} \quad \text{and} \quad D_{eff} = \frac{\varepsilon_p D_m}{\tau}$$

In the above equations, D_m is a molecular diffusion coefficient (m^2/s), k_{ext} is an external mass transfer coefficient (m/s), d_p is a particle diameter (m), and τ is a tortuosity parameter.

Eq. (4) was used with success for modeling peak profiles eluted from columns packed with a totally porous adsorbent, under strongly non-isothermal retention conditions [11].

Following the method presented in [10] and taking into account that the number of theoretical plates, N, calculated by the method of moments, for Eq. (1) is given by [6]:

$$\frac{1}{N} = \frac{2D_L s_e}{uL} + 2\left(\frac{k_1}{1+k_1}\right)^2\frac{ud_p}{\varepsilon_e L F_e 6}\left[\frac{d_p}{10D_{eff}}\frac{1+2\rho+3\rho^2-\rho^3-5\rho^4}{(1+\rho+\rho^2)^2} + \frac{1}{k_{ext}}\right] \quad (5)$$

with the parameter k_1 defined as

$$k_1 = F_e\left(\varepsilon_p + (1-\varepsilon_p)\frac{\partial q}{\partial c}\right)(1-\rho^3),$$

it is easy to obtain the expression for the apparent axial dispersion $D_{a,x}$ coefficient for columns packed with a core–shell adsorbent:

$$D_{a,x} = \frac{D_L\varepsilon_e}{\varepsilon_t} + \left(\frac{k_1}{1+k_1}\right)^2\frac{u^2 d_p}{\varepsilon_t\varepsilon_e F_e 6}\left[\frac{d_p}{10D_{eff}}\frac{1+2\rho+3\rho^2-\rho^3-5\rho^4}{(1+\rho+\rho^2)^2} + \frac{1}{k_{ext}}\right] \quad (6)$$

2.1.1. Isotherm equation

The mass balance model must be combined with an appropriate isotherm equation. In this work, we consider a linear isotherm where Henry constant, H, is a function of the local temperature and pressure. Hence, the isotherm model is given by [2,9,12]:

$$q = c\cdot H = c\cdot H_o\,\exp\left(-\frac{E}{RT}\right)\exp\left(-\Delta V_m\frac{P-P_{ref}}{RT}\right) \quad (7)$$

where H_o is the isotherm parameter, T is the temperature, E is the activation energy of adsorption, R is the universal gas constant, ΔV_m is the difference between the partial molar volumes of the solute in the adsorbed layer and in the liquid phase and p, p_{ref} are the pressure and reference pressure, respectively.

2.2. Methods of calculation of the physico-chemical parameters for the mass balance equations

To solve the mass balance presented above, the external mass transfer coefficient, k_{ext}, the axial dispersion coefficient, D_L, the axial and radial apparent dispersion coefficient, $D_{a,x}$, $D_{a,r}$, the molecular diffusivity, D_m, and the tortuosity parameter, τ, must be calculated. In this work, the external mass transfer coefficient k_{ext} was calculated from the Wilson and Geankoplis [13] correlation:

$$Sh = \frac{1.09}{\varepsilon_e}Re^{0.33}Sc^{0.33} \quad (8)$$

where

$$Sh = \frac{k_{ext} d_p}{D_m}, \quad Re = \frac{u \rho d_p}{\eta}, \quad Sc = \frac{\eta}{\rho D_m}$$

The parameters η and ρ are the local (at position x, r) mobile phase viscosity and density, respectively.

The local dispersion coefficient D_L was calculated from the relationship [12]:

$$D_L = \gamma_1 D_m + \gamma_2 u d_p \tag{9}$$

where γ_1 and γ_2 are geometrical constants. It was assumed that $\gamma_1 = 0.7$ [12], whereas γ_2 was estimated from the experimental data.

The local value of the molecular diffusion coefficient D_m was estimated from the Wilke–Chang equation [14].

We need also the apparent dispersion coefficients. The local value of the axial dispersion coefficient was calculated from Eq. (6) and radial dispersion coefficient, $D_{a,r}$, was calculated on the base of the plate height equation derived by Knox [9,15,16].

$$D_{a,r} = \frac{0.03 d_p u}{\varepsilon_t} + 0.07 D_m \tag{10}$$

The tortuosity parameter, τ, was calculated from the correlation [17]:

$$\tau = \varepsilon_p + 1.5(1 - \varepsilon_p) \tag{11}$$

2.3. Method of calculation of numerical solutions of the models

The mass balance equation coupled with the heat balance equation was solved with the method described previously in details in [8,9]. Namely, first the steady-state distributions of the temperature and pressure profiles were derived. As a boundary condition for the heat balance at the outer radius of the column, the wall temperature profile measured in [2] was used. Namely, the experimental temperature was interpolated by a suitable polynomial and the wall temperature was calculated from this polynomial. Afterwards the time dependent mass balance equation was solved using the temperature and the pressure obtained earlier.

3. Experimental

The experiments were described in detail by Gritti and Guiochon [2]. In this work we interpret the results obtained with pure acetonitrile used as the mobile phase. The analyte was naphtho[2,3-α]pyrene, purchased from Aldrich (Milwaukee, WI, USA).

A 1.7 μm BEH-C18 column (150 mm × 2.1 mm, from Waters, Milford, MA, USA) and a 1.7 μm Kinetex-C18 (150 mm × 2.1 mm, from Phenomenex, Torrance, CA, USA) column were used. The total porosity of the BEH column was 0.627, its external porosity 0.382 and the particle porosity 0.396. For the Kinetex column the total porosity was 0.517, the external porosity 0.409 and the shell particle porosity 0.29.

The injected volume was 1 μl and the concentration was kept about 0.1 g/l to operate with a linear adsorption isotherm. The peak profiles were obtained for several mobile phase velocities, at wavelength 294 nm. For the calculations we chose velocities equal 0.28, 0.56, 0.8, 1.0 and 1.1 ml/min.

4. Results and discussion

In this work we applied the mass transfer model presented above for the interpretation of the efficiencies measured for the columns packed with particles having the same nominal diameter but either totally porous or with an inert core. To solve this mass transfer model, the values of the physic-chemical parameters were calculated in local column position as was stated previously. Instead of the nominal diameters of the particles of adsorbent, the measured diameters were used [2]: for BEH $d_p = 1.77$ μm, for Kinetex $d_p = 1.89$ μm and $R_i/R_e = 0.72$.

4.1. The thermal conductivity

The thermal conductivity of a porous medium impregnated with a liquid depends on the geometry of the solid bed, on its porosity, and on the thermal properties of the different components of the medium [18]. For two-component heterogeneous system that has a chaotic structure, Zarichnyak et al. [19] proposed the following equation for the calculation of the effective conductivity

$$\lambda_{eff} = \varepsilon_t^2 \lambda_{elu} + \varepsilon_s^2 \lambda_s + 4 \varepsilon_t \varepsilon_s \frac{\lambda_{elu} \lambda_s}{\lambda_{elu} + \lambda_s} \tag{12}$$

where the porosity ε_s is the ratio of the volume of the solid phase in the bed to the geometrical volume of the column and λ_s, λ_{elu} are the solid phase and the eluent conductivity, respectively.

The thermal conductivities of non-porous silica, solid octadecane and liquid acetonitrile were taken as 1.4, 0.35 and 0.203 W/m/K, respectively [2]. To calculate the effective conductivity of the bed, Eq. (12) was used first to calculate the effective conductivity of the solid matrix (which is composed of porous silica and the C_{18} ligands bonded to the silica surface) $\lambda_{s,ef}$. Next, the effective conductivity was obtained from $\lambda_{s,ef}$ and λ_{elu}. For the BEH column λ_{eff} was equal 0.366 and for the Kinetex column 0.502 W/m/K.

4.2. Parameters of isotherm equation

The parameters of the isotherm model, Eq. (7) are the activation energy of adsorption, E, the molar volume change, ΔV_m, and the enthalpy limit, H_o, which was estimated as follows.

For smallest velocity, the value of H_o was calculated from the equation:

$$H_o = \frac{H_{low}}{\exp\left(-\frac{E}{RT_{av}}\right) \exp\left(-\Delta V_m \frac{P_{av} - P_{ref}}{RT}\right)} \tag{13}$$

where the T_{av} and P_{av} are the average temperature and pressure inside the column, calculated for the lowest mobile phase velocity and H_{low} is the experimental value of the Henry constant calculated for the lowest mobile phase velocity from Eq. (14) or (15).

The Henry constant for fully porous particles, was calculated from the following equation:

$$H = \frac{\varepsilon_t}{1 - \varepsilon_t} \left(\frac{t_r u_{av}}{L \varepsilon_t} - 1 \right) \tag{14}$$

and, for shell particles, from expression:

$$H = \left(\frac{t_r u_{av}}{s_t L} - 1 \right) \frac{\varepsilon_t}{1 - \varepsilon_e} (1 - \varepsilon_p)(1 - \rho^3) \tag{15}$$

where u_{av} is the average velocity, and t_r the retention time.

Eq. (7) coupled with Eq. (13) was the isotherm model used for the estimation of the two parameters $-E$ and $-\Delta V_m$. These parameters were estimated with the trial and error method, to obtain good agreement of the retention times between the experimental and calculated peaks obtained for the lowest and highest flow rates.

The values of the parameter H_o were 4.07 and 3.32 for BEH-C_{18} and Kinetex-C_{18} column, respectively. The values of the molar volume change, ΔV_m, were −1.516E−6 l/mol and −2.17E−9 l/mol for the BEH-C_{18} and Kinetex-C_{18} columns, respectively. The values of the activation energy of adsorption, E, were −21,290 J/mol and −16,000 J/mol for the BEH-C_{18} and Kinetex-C_{18} columns, respectively.

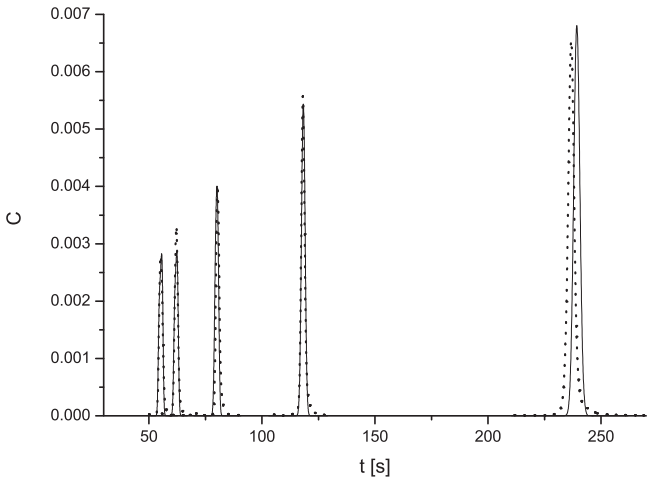

Fig. 1. Comparison of the experimental (dotted lines) and theoretical (solid lines) concentration profiles of naphtho[2,3-α]pyrene. Column 150 mm × 2.1 mm BEH-C_{18}, F_v = 1.1, 1.0, 0.8, 0.56 and 0.28 ml/min (from left to right).

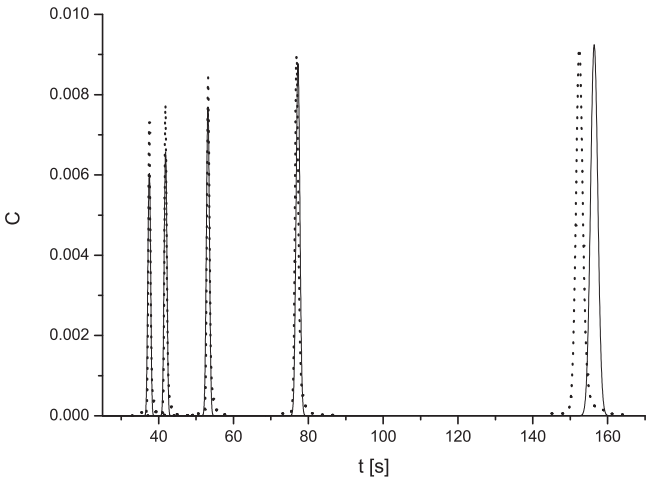

Fig. 2. Comparison of the experimental (dotted lines) and theoretical (solid lines) concentration profiles of naphtho[2,3-α]pyrene. Column 150 mm × 2.1 mm Kinetex-C_{18}, F_v = 1.1, 1.0, 0.8, 0.56 and 0.28 ml/min (from left to right).

4.3. Comparison of the experimental and theoretical peak profiles

Peak broadening is caused by two groups of effects: (i) the mass transfer resistances and axial and radial dispersion and (ii) the gradient of the mobile phase velocity and the gradient of the retention coefficient, which both result from the temperature gradients across the column. The second effect is decreasing to zero when the column becomes nearly isothermal. On the other hand it becomes the most important for large temperature gradients across the column. Dispersion due to the second group of effects is accounted automatically by the two-dimensional mass balance equation (2).

Dispersion caused by the first group of effects can be modeled by introducing the apparent axial and radial dispersion coefficients. To obtain a good agreement between the theoretical and the experimental peak profiles, the value of the apparent axial dispersion coefficient is typically estimated from the experimental data, for each mobile phase velocity, separately. This drawback can be, to some degree, overcome by calculating the axial apparent dispersion coefficient from Eq. (6) and all the other parameters, but γ_2, from the correlations presented in Section 2.2. The γ_2 parameter should be estimated for the conditions for which the temperature gradient inside column is smallest – it means for such experimental conditions that the first group of effects dominates peak broadening.

The value of the γ_2 parameter was estimated for each column, at the smallest mobile phase velocity, 0.28 ml/min, and the same value of the γ_2 was used for the simulation of the peak profiles at all the other velocities.

The values obtained for γ_2 were 2.5 and 2.8 for the BEH-C_{18} and the Kinetex-C_{18} columns, respectively.

Comparisons between the experimental and the calculated peak profiles are shown in Figs. 1 and 2. For a mobile phase flow of 0.28 ml/min, the theoretical profiles are shifted toward longer retention times, for both columns. The discrepancy between the calculated and experimental retention times decreases with increasing mobile phase velocity. The relative errors between the predicted and measured retentions time are less than 1.3% and 2.6% for the BEH-C_{18} and the Kinetex-C_{18} columns, respectively.

For all the mobile phase flow rates, the calculated peak profiles are slightly lower than those measured, except for the profile for which the γ_2 parameter was matched. However, in our opinion, the accuracy of the peak shape prediction is satisfactory.

4.4. The Van Deemter plots

Fig. 3 shows the plots of the reduced height equivalent to a theoretical plate, h = HETP/d_p of naphtho[2,3-α]pyrene on both columns. The HETP for the experimental data were calculated with the help of the EMG (Exponentially Modified Gaussian) [20] function. The experimental peaks profiles were approximated by an EMG function and afterwards, on the basis of this function, the experimental HETP = L/N were calculated using the method of moments:the first moment:

$$\mu_1 = \frac{\int C(t)t\,dt}{\int C(t)dt} \tag{16}$$

the second central moment:

$$\mu_2' = \frac{\int c(t)(t-\mu_1)^2 dt}{\int c(t)dt} \tag{17}$$

and the relation between the number of theoretical plates and these moments:

$$N = \frac{\mu_1^2}{\mu_2'} \tag{18}$$

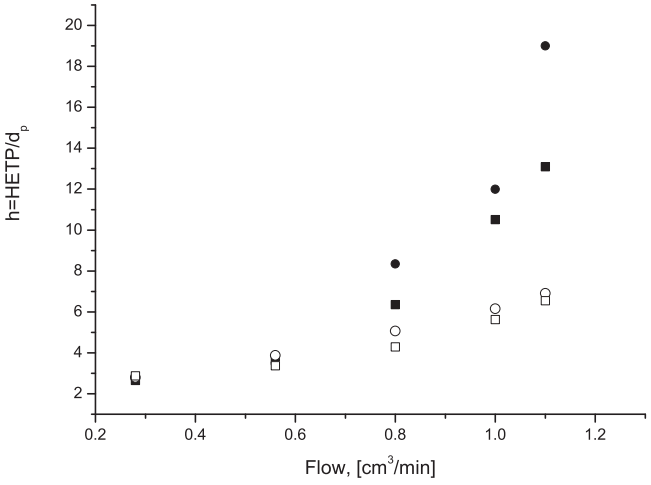

Fig. 3. Comparison between the reduced HETP for experimental (round symbols) and calculated (square symbols) peak profiles. BEH column – solid symbols; Kinetex column – open symbols.

Also the theoretical values of the HETP were calculated by the method of moments applied to the simulated band profiles.

Generally, the h values for the experimental peak profiles are higher than those for the calculated profiles. This is related to the influence of the small tails clearly visible in the rear parts of the experimental peaks profiles. However, the changes of the plots of the column efficiency versus the mobile phase flow are well reproduced. The reduced HETP of the Kinetex column remains larger than that of the BEH column in the velocity range 0.2–0.6 cm^3/min. For higher velocities, the loss in column efficiency increases faster for the BEH column. This is related to the higher radial temperature gradient observed in the BEH column. For example, the calculated temperature gradient at the column outlet, for the highest flow rate was 1649.5 K/m for the BEH column and 1057 K/m for the Kinetex column. This difference is explained by the higher effective thermal conductivity of a column filled with shell adsorbent.

4.5. Influence of the inert-core thermal conductivity on the HETP

As shown above, for large mobile phase velocities, the efficiency of the column packed with shell particles, is higher than that of the column packed with totally porous particles. To investigate the influence of the inert-core thermal conductivity on the efficiency of the column, we made some assumptions and solved the coupled mass balance and heat balance equations, presented above. First, we assumed that the columns have the same geometrical parameters as the Kinetex column, meaning the same column length, diameter, external, internal, particle porosities, particle and inert core radius as those of the Kinetex column. Next, we assumed that the core of the shell particles is made of materials with different values of the thermal conductivity: silica (λ = 1.4 W/m/K), zirconium (λ = 2 W/m/K), alumina (λ = 40 W/m/K), and gold (λ = 320 W/m/K) and of hypothetical materials with λ = 15 and λ = 25 W/m/K. The effective conductivity, λ_{eff}, of the particles with inert-core made of silica, zirconium, hypothetical materials, alumina and gold, are 0.502, 0.616, 2.89, 4.628, 7.23 and 55.77 W/m/K, respectively; they were calculated using Zarichnyak et al. equation [19], as described in Section 4.1. In this case, to solve the heat balance equation, we could not use the measured wall temperature as a boundary condition at the outer radius of the column. However, we could not ignore the temperature distribution in the steel wall of the column. So, we solved the heat transfer equations for the mobile phase and the wall as explained in [8]. The temperature distribution in the steel wall of the column was calculated for different heat transfer coefficient, h_e. For h_e, equal to 60 we obtained a good agreement between the calculated and the measured temperature distribution along the Kinetex column wall. This estimated value of the heat transfer coefficient was used with all subsequent simulation. The heat transfer by radiation was ignored.

For each temperature distribution obtained using the values of the thermal conductivity assumed above, the mass balance equation was solved. The values of the isotherm parameters H_o, ΔV_m, and E, were assumed as before to be equal to 3.32, −2.17E−9 l/mol and −16,000 J/mol, respectively.

Fig. 4 compares the calculated peak profiles of naphtho[2,3-α]pyrene for different inert-core materials, for a mobile phase velocity of 1.1 ml/min. The theoretical value of the HETP was calculated by the method of moments applied to the simulated band profiles. As can be seen, the retention times increase with increasing effective conductivity and decreasing overall heat transfer resistances. As a result, the average column temperature decreases and the retention factor increases.

The dependence of the h = HETP/d_p on the thermal conductivity of the inert-core is shown in Fig. 5. At the beginning (for low thermal conductivity), the efficiency of the column increases. However, for

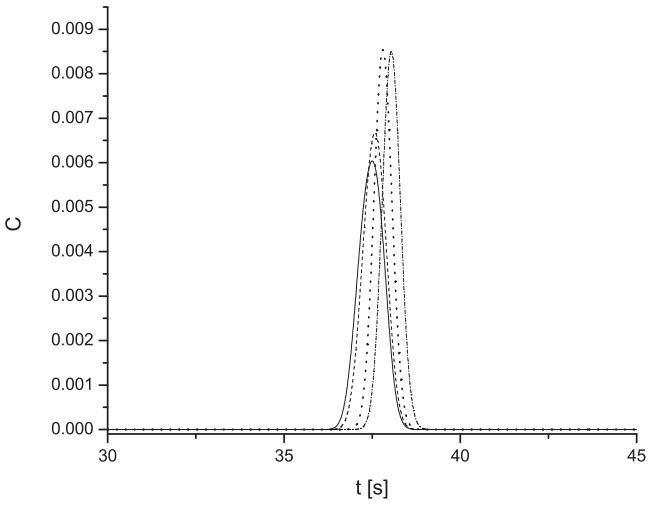

Fig. 4. Comparison of the theoretical concentration profiles of naphtho[2,3-α]pyrene for different inert-core materials: silica (solid line), zirconium (dashed line), alumina (dotted line) and gold(dashed-dotted line). Column 150 mm × 2.1 mm, F_v = 1.1 ml/min.

λ equal to about 30–40 W/m/K, the column efficiency reaches its maximum value.

The lost of column efficiency is directly connected with the radial temperature distribution. In the cases studied, the radial temperature gradients at the column outlet were 1150, 952, 276, 209, 169, and 114 K/m for silica-, zirconium-, the hypothetical materials, alumina- and gold-core, respectively. This means that a radial temperature gradient less than about 170 K/m has little influence on the column efficiency.

4.6. Influence of the decreasing effective thermal conductivity on the peaks profiles

In the previous section we proved that the column efficiency increases with increasing effective thermal conductivity. In this section, for illustrative purposes, we analyzed band profiles calculated for decreasing effective thermal conductivity. The calculations were performed for BEH and for Kinetex-like columns. The values of the parameters of the isotherm model were the same as those used previously in both cases. The geometry of the adsorbent, the

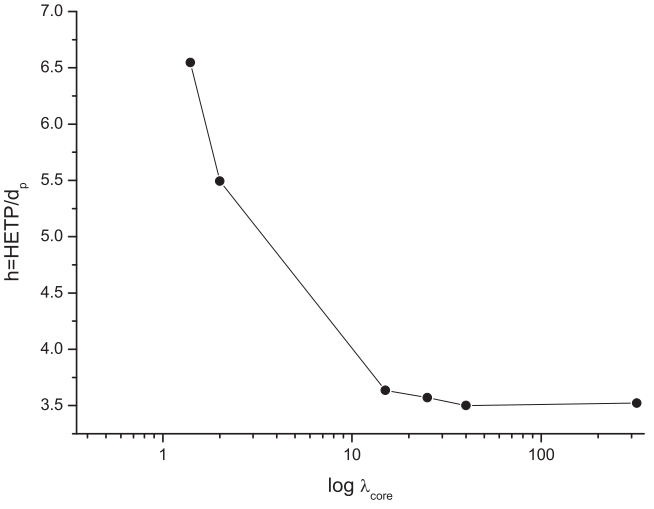

Fig. 5. Calculated dependence of the h on the thermal conductivity of the inert-core. The solid symbols depict the column efficiency calculated for silica, zirconium, hypothetical materials, alumina and gold, from left to right.

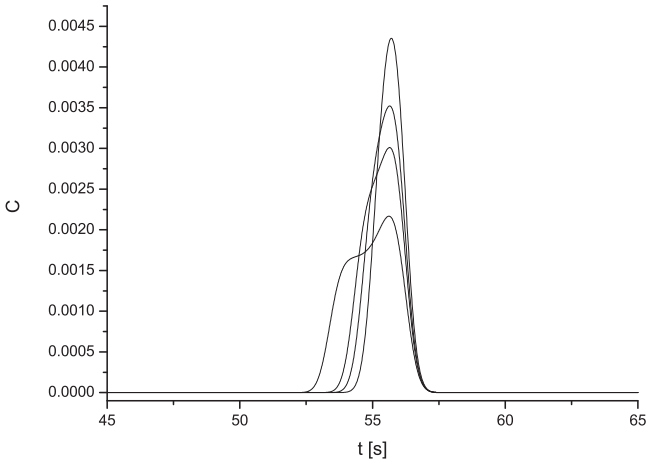

Fig. 6. Comparison of the theoretical concentration profiles of naphtho[2,3-α]pyrene for different effective thermal conductivities of the bed equal to: 0.25, 0.40, 0.50, and 0.7 W/m/K, from the smallest to the highest band profiles. Column BEH, 150 mm × 2.1 mm, F_v = 1.1 ml/min.

particles and the bed porosities were assumed to be the same as for the BEH and the Kinetex columns. Only the effective thermal conductivity of the core of the shell particles was changed. The results of the simulations made for the BEH and the Kinetex-like columns at the flow rate F_v = 1.1 ml/min with assumed effective thermal conductivities of the bed equal to: 0.25, 0.40, 0.50, and 0.7 W/m/K, are illustrated in Figs. 6 and 7.

As can be seen, for both columns, the peaks become wider and smaller with decreasing effective thermal conductivity. When this conductivity is further decreased, the peak begins to split. This spectacular effect results directly from the increase of the radial thermal gradient due to the decreasing effective thermal conductivity.

Theoretically, a decrease of the effective conductivity, unfavorable for the column efficiency, can take place when a mobile phase with a lower conductivity is applied or when the conductivity of the adsorbent solid matrix is decreased. The hypothetical solid phase or eluent conductivity giving effective thermal conductivities equal to 0.25, 0.40, 0.50 and 0.70 W/m/K are presented in Tables 1 and 2. Taking into account the conductivities of the liquid phase used in chromatography (water – 0.58, methanol – 0.21, acetonitrile – 0.2, n-propanol – 0.15 W/m/K, for T = 25 °C) it is seen that the probability

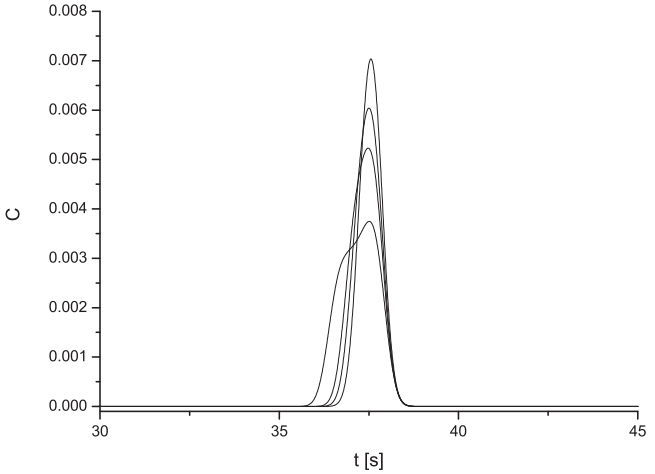

Fig. 7. Comparison of the theoretical concentration profiles of naphtho[2,3-α]pyrene for different effective thermal conductivities of the bed equal to: 0.25, 0.40, 0.50, and 0.7 W/m/K, from the smallest to the highest band profiles. Column Kinetex, 150 mm × 2.1 mm, F_v = 1.1 ml/min.

Table 1
The hypothetical solid phase or eluent conductivity for Kinetex column.

λ_s	λ_{elu}	λ_{eff}[a]
0.308		0.25
0.895	0.203[a]	0.40
1.4		0.50
2.46		0.70
	–	0.25
1.4[a]	0.106	0.40
	0.203	0.50
	0.424	0.70

[a] Assumed values.

Table 2
The hypothetical solid phase or eluent conductivity for BEH column.

λ_s	λ_{elu}	λ_{eff}[a]
0.36		0.25
1.85	0.203[a]	0.40
3.2		0.50
6.1		0.70
	0.097	0.25
1.4[a]	0.238	0.40
	0.345	0.50
	0.595	0.70

[a] Assumed values.

of peak splitting is greater for a column packed with a totally porous adsorbent, such as BEH. For example, the thermal conductivity of the mobile phase should be less than zero for a column packed with a Kinetex like adsorbent to obtain an effective conductivity equal to 0.25 (assuming the validity of Zarichnyak correlation).

On the other hand, the conductivity of the real adsorbent matrix material is rather too high for peak splitting to be possible for a Kinetex like adsorbent.

5. Conclusions

In this work we have compared the efficiency of columns packed with different kinds of particles – totally porous particles and core–shell particles. The numerical solutions of the proposed mathematical model gave theoretical elution peak profiles for both columns. We compared the plots of the reduced heights equivalent to a theoretical plate, h, of naphtho[2,3-α]pyrene on a Kinetex and a BEH columns for the experimental and the calculated peak profiles. The results of this comparison confirm a suggestion formulated earlier [2] that the smaller loss of efficiency observed for columns packed with superficially porous shell particles with increasing flow rates is caused by the higher effective conductivity of these columns. From this analysis of the influence of the solid-core conductivity on the column efficiency, it follows that the efficiency of 2.1 mm i.d. columns packed with shell particles reaches a maximum when the solid-core conductivity is greater than about 30–40 W/m/K.

Acknowledgments

This work was partially supported by grant no. N204 002036 of the Polish Ministry of Science and Higher Education. Financial support from the European Social Fund, Polish National Budget, Podkarpackie Voivodship Budget (within Sectoral Operational Program Human Resources) "Wzmocnienie instytucjonalnego systemu wdrazania Regionalnej Strategii Innowacji w latach 2007-2013" is gratefully acknowledged.

References

[1] http://www.advanced-materials-tech.com/halo.html, 2007.

[2] F. Gritti, G. Guiochon, J. Chromatogr. A 1217 (2010) 5069.
[3] F. Gritti, I. Leonardis, D. Shock, P. Stevenson, A. Shalliker, G. Guiochon, J. Chromatogr. A 1217 (2010) 1589.
[4] F. Gritti, I. Leonardis, J. Abia, G. Guiochon, J. Chromatogr. A 1217 (2010) 3819.
[5] E. Oláh, S. Fekete, J. Fekete, K. Ganzler, J. Chromatogr. A 1217 (2010) 3642.
[6] K. Kaczmarski, G. Guiochon, Anal. Chem. 79 (2007) 4648.
[7] K. Kaczmarski, J. Chromatogr. A 1218 (2011) 951.
[8] K. Kaczmarski, J. Kostka, W. Zapała, G. Guiochon, J. Chromatogr. A 1216 (2009) 6560.
[9] K. Kaczmarski, F. Gritti, J. Kostka, G. Guiochon, J. Chromatogr. A 1216 (2009) 6575.
[10] D. Antos, K. Kaczmarski, W. Piatkowski, A. Seidel-Morgenstern, J. Chromatogr. A 1006 (2003) 61.
[11] J. Kostka, F. Gritt, G. Guiochon, K. Kaczmarski, J. Chromatogr. A 1217 (2010) 4704.
[12] G. Guiochon, A. Felinger, A.M. Katti, D. Shirazi, Fundamentals of Preparative and Nonlinear Chromatography, second ed., Elsevier, Amsterdam, 2006.
[13] E.J. Wilson, C.J. Geankoplis, Ind. Eng. Chem. Fundam. 5 (1966) 9.
[14] C.R. Wilke, P. Chang, AlChE J. 1 (1955) 264.
[15] D. Horne, J.H. Knox, L. McLaren, Separ. Sci. 1 (1966) 531.
[16] J.H. Knox, G.R. Laird, P.A. Raven, J. Chromatogr. 122 (1976) 129.
[17] M. Suzuki, Adsorption Engineering, Elsevier, Amsterdam, 1990.
[18] R.B. Bird, W.E. Stewart, E.N. Lightfoot, Transport Phenomena, John Wiley & Sons, 2002.
[19] Y.P. Zarichnyak, V.V. Novikov, Inzhenerno-Fizicheskii Zhurnal 34 (1978) 648.
[20] A. Felinger, Data Analysis and Signal Processing in Chromatography, Elsevier, 1998.